Molecular Printing

Deutsche Ausgabe: DOI: 10.1002/ange.201505150
Internationale Ausgabe: DOI: 10.1002/anie.201505150

On-Tip Photo-Modulated Molecular Printing

Zhuang Xie, Yu Zhou, James L. Hedrick, Peng-Cheng Chen, Shu He, Mohammad M. Shahjamali, Shunzhi Wang, Zijian Zheng, and Chad A. Mirkin**

Abstract: *The concept of using cantilever-free scanning probe arrays as structures that can modulate nanoscale ink flow and composition with light is introduced and evaluated. By utilizing polymer pen arrays with an opaque gold layer surrounding the base of the transparent polymer pyramids, we show that inks with photopolymerizable or isomerizable constituents can be used in conjunction with light channelled through the pyramids to control ink viscosity or composition in a dynamic manner. This on-tip photo-modulated molecular printing provides novel chemically and mechanically controlled approaches to regulating ink transport and composition in real time and could be useful not only for rapidly adjusting feature size but also for studying processes including photoreactions and mass transport at the nanoscale, self-assembly, and cell–material interactions.*

Emerging forms of scanning probe lithography (SPL) are transforming the field by creating rapid and straightforward ways of generating nanostructures on surfaces with remarkable control over feature size, shape, and composition.[1] Such techniques have enabled breakthroughs in a wide variety of fields spanning combinatorial synthesis and screening[2] to the fabrication of photonic and plasmonic nanostructures[3] to chip-based bioassays and medical diagnostics.[4] Typically, two conceptually different strategies are involved in SPL: one class of tools focuses on the delivery of energy to a resist layer to induce localized physical and/or chemical changes such as STM lithography,[5] beam pen lithography,[6] nanografting,[7] local anodic oxidation and related electrochemical approaches,[8] and the other class of tools involves the direct transfer of "ink" such as dip-pen nanolithography (DPN),[9] scanning probe block copolymer lithography (SPBCL),[10] polymer pen lithography (PPL),[11] and hard-tip, soft-spring lithography (HSL).[12] Others such as dip-pen nanodisplacement lithography (DNL)[13] and thermal DPN[14] combine elements of both strategies. Collectively, these tools allow one to make and manipulate a wide variety of nanostructures on surfaces with sub-100 nm resolution.

With the advent of cantilever-free scanning probe arrays,[6,11,12,15] researchers can pattern large areas at very low cost without sacrificing resolution or materials flexibility. Such structures typically consist of elastomeric arrays of pyramids, mounted on a hard transparent backing, which span macroscopic areas; when utilized with a conventional atomic force microscope (AFM), they can be used to either transport molecules from their tips to surfaces[11,16] or channel light and effect patterning with near-field or far-field resolution.[6,17] When molecules are transported from the tip to surface, one typically relies on contact time or force to control feature size.[11,18] However, by combining energy transfer (controlled with photons) with molecular transfer, one in principle could gain a new level of control. Herein, we show how a cantilever-free architecture can be designed to allow one to utilize light to chemically regulate the flow of molecule-based materials from tip to surface (Figure 1). It does so via two different pathways. The first involves a controlled light-induced polymerization that only occurs on the surfaces of the pyramids that define the tips; polymerization leads to

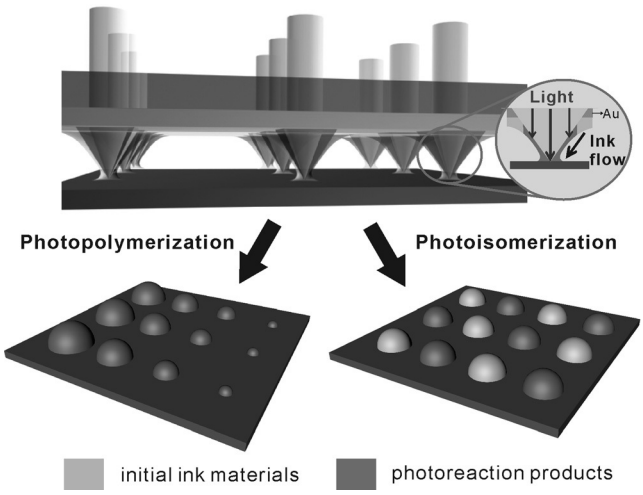

Figure 1. Illustration of on-tip photo-modulated molecular printing in which nanoscale photoreactions are induced on the surface of pyramids by light illumination from the backside of the array. Photocontrol of ink transport and chemical composition of the printed features are effected by exploiting either photopolymerization (left) or photoisomerization (right) of ink molecules.

[*] Dr. Z. Xie,[+] S. He, Dr. M. M. Shahjamali, S. Z. Wang, Prof. C. A. Mirkin
Department of Chemistry and International Institute for Nanotechnology, Northwestern University
2145 Sheridan Road, Evanston, IL 60208 (USA)
E-mail: chadnano@northwestern.edu
Dr. Z. Xie,[+] Prof. Z. J. Zheng
Nanotechnology Center, Institute of Textiles and Clothing, The Hong Kong Polytechnic University, Hong Kong SAR (China)
E-mail: tczzheng@polyu.edu.hk
Y. Zhou,[+] P.-C. Chen, Prof. C. A. Mirkin
Department of Materials Science and Engineering, Northwestern University, 2220 Campus Drive, Evanston, IL 60208 (USA)
J. L. Hedrick, Prof. C. A. Mirkin
Department of Chemical and Biological Engineering, Northwestern University, 2145 Sheridan Road, Evanston, IL 60208 (USA)
[+] These authors contributed equally to this work.

Supporting information for this article is available on the WWW under http://dx.doi.org/10.1002/anie.201505150.

increased ink viscosity and decreased flow rate. The second approach uses light to dynamically toggle between two different isomeric ink forms, allowing one to change the type of molecules transported in an experiment in real time, without the need to change the array or inking procedure. Notably, the photo-modulation method is remarkably simple and straightforward to implement, and the position and intensity of the delivered light can be easily manipulated with high precision and rapid switching for site-selective control over multiple length scales.[6]

In order to effect photochemical regulation of ink flow on the surface of pyramidal tips, polymer pen arrays made of hard polydimethylsiloxane (PDMS)[11] were coated with an opaque layer of gold in the areas surrounding the base of the pyramids as well as the flat backplane, while the pyramidal tips were unmodified and maintained as transparent apertureless pen arrays.[17b] When the backside of the array is illuminated during printing, light moves through the pyramids and is focused at the tips, which can drive photoreactions of photosensitive ink materials on the tip. A UV-curable liquid photopolymer (NOA 81, Norland Products, Inc.) was chosen as the ink material for an initial proof-of-concept study. When exposed to UV light, the NOA ink undergoes a thiol–ene photopolymerization between trimethylolpropane tris(3-mercaptopropionate) and urethane-containing tetrafunctional allyl ether,[19] which will result in an increase in ink viscosity and a concomitant decrease in ink transport rate from tip to surface. To test the ability to use this reaction to modulate ink transport, an apertureless pen array (8×5 mm^2, 4000 pyramidal pens, each pen with a 40×40 μm base, 100 μm pitch) was inked with the NOA ink by spin coating, and then attached to a piezoelectric scanner part of a scanning probe system (XE-150, Park Systems). After leveling the 2D pen array with respect to a silicon wafer substrate,[11] the pen array was brought into contact with the substrate and used to create a pattern consisting of 160000 dots of deliberately varied size, with each pen generating an 8×5 dot array. The dwell time was 5 s under ambient conditions. During patterning, a portion of the backside of the pen array was illuminated with UV light (365 nm, ≈0.1 mW cm^{-2}) by using a focusing lens (3 mm diameter). The remainder of the pen array (≈33 mm^2) was not illuminated and used as a control. After patterning, there was a significant difference between the features printed with and without UV illumination, as observed by optical microscopy. In the area under continuous UV illumination, the printed NOA features exhibited a gradual decrease in feature size (dot diameter) along the writing direction (left to right and top to bottom), while the feature sizes were near-identical for those printed in the dark (Figure 2A). Further AFM characterization confirmed that immediately after turning on the UV light, feature volume could be reduced deliberately by a factor of >1000, while feature size could be reduced from 1.8 μm to 150 nm upon 18 min of illumination (Figure 2B and C). This light-induced decrease in feature size is a direct result of the increase in ink viscosity that accompanies polymerization, which has been characterized for bulk samples in the literature.[19b] The influence of solvent and environmental humidity is negligible since the NOA ink is solvent-free and impermeable to water vapor.

Next, we investigated how the ink transport rate varied with the extent of photopolymerization by examining the

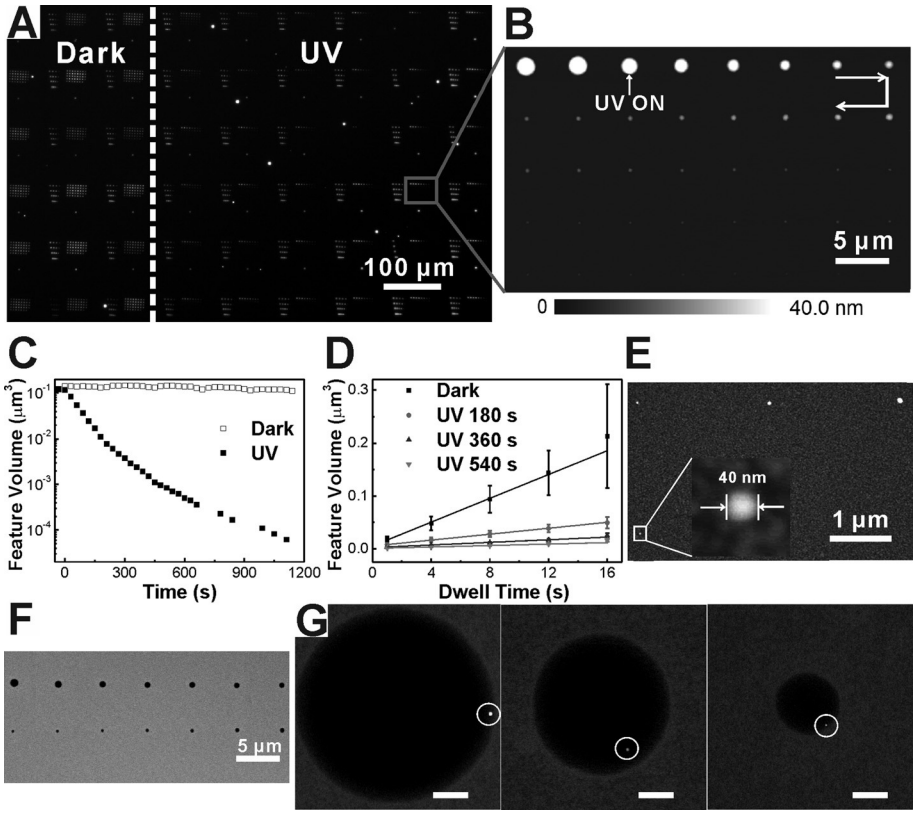

Figure 2. Photo-modulated ink transport by polymerization. A) Dark-field optical microscope image of the printed features of NOA ink under dark (left) and UV illumination (right) conditions. B) Atomic force microscopy (AFM) image of a typical NOA dot array patterned under UV illumination (365 nm, ≈0.1 mW cm^{-2}), with the white arrows showing the writing direction. C) Plot of feature volume with time for two typical arrays patterned under dark and UV light. D) Dwell-time dependence of the NOA feature volume with varied UV illumination time. E) AFM image of NOA dot features generated on gold substrate with size ranging from 100 to 40 nm by a 15 min UV illumination. F) Scanning electron microscope (SEM) image of a typical dot array of PEGDA/PEO-*b*-P2VP/$HAuCl_4$ ink printed under UV illumination (365 nm, ≈50 mW cm^{-2}). G) Magnified SEM images of the patterned polymer spots with single gold nanoparticles inside as indicated by the white cycles. From left to right, the polymer feature size was 1100, 760, and 325 nm, corresponding to 19, 15, and 8 nm diameter nanoparticles, respectively. Scale bars: 200 nm.

time-dependent ink deposition under UV illumination. NOA dot arrays were patterned at different UV illumination times from 0 to 540 s. For each UV illumination time, the dwell time was varied from 1 to 16 s (Figure S1A in the Supporting Information). By plotting the volume of printed features with the dwell time under different UV illumination times, it is clear that ink deposition rate decreases with increasing UV illumination (Figure 2D and S1), which is consistent with previous reports on viscosity-dependent transport of polymer inks.[14b,20] Indeed, techniques like thermal DPN utilize thermally-induced phase changes in a solid ink to effect transport,[14b] while other ink matrix approaches use predefined combinations of different polymers to effect ink transport.[20] The former requires a heating apparatus, and since heat dissipation is inherently slow, it makes it difficult to precisely and rapidly control ink flow; the latter is cumbersome as it requires making a new ink mixture every time one wants to effect a change. The photochemical approach described herein offers a straightforward way to spatially, temporally, and independently control ink properties while the ink resides on individual tips within an array.

Since the photopolymerization of the ink molecules at the tip can be finely tuned, this photochemical approach allows one to control feature size regardless of the initial ink viscosity, environmental humidity, and ink loading. As shown in Figure 2E, we have made NOA features with diameters ranging from 100 to 40 nm on gold substrates using continuous UV illumination ($\approx 0.1\ mW\,cm^{-2}$) over a 15 min time period and a dwell time of 5 s. Under these conditions (note that at low intensities light fluctuations occur from use to use), here irradiating beyond 15 min resulted in the complete solidification of ink on the tip and the inability to transfer the ink molecules to the substrate. The 40 nm feature size is notable (Figure 2E), since prior to these studies, 60 nm is the smallest reported feature size by PPL. In principle, resolution can be further increased by adjusting the force-dependent tip deformation[15c] and ink–substrate interactions.[21] Moreover, the on-tip photopolymerization strategy as compared with conventional PPL of liquid inks (in the dark) provides an enhancement in feature size uniformity with the standard deviation in feature size decreasing from 17 to 8–11%, depending on illumination time (Figure S2). This is a result of greater control over ink transport rate; as the ink viscosity increases, it becomes the dominant factor in determining the ink transport rate, which can be precisely controlled at each tip with light.

Light-induced polymerization is not limited to the thiol–ene based chemistry of the NOA ink. Indeed, it can be universally applied to a wide range of photoreactive ink materials to control ink transport. For example, a diacrylate monomer polyethylene glycol diacrylate (PEGDA, average $M_n = 700$) was mixed at a 1 to 1 volume ratio with an aqueous solution of poly(ethylene oxide)-block-poly(2-vinyl pyridine) (PEO-*b*-P2VP) loaded with $HAuCl_4$ to create a photopolymerizable ink. The photo-induced (365 nm) free-radical polymerization of PEGDA modulates the ink viscosity of the mixture and resulting transport rates. The resulting feature volumes can be precisely controlled and used to adjust the number of metal ions within them. This technique is called scanning probe block copolymer lithography (SPBCL),[10,20c–d] and subsequent thermal treatment of the features can be used to generate a single crystalline nanoparticle within each feature. As proof-of-concept, the PEGDA and PEO-*b*-P2VP/$HAuCl_4$ ink mixture was patterned onto a hexamethyldisilazane (HMDS) modified silicon substrate under continuous UV illumination ($\approx 50\ mW\,cm^{-2}$) and a 5 s dwell time. Again, the resulting feature diameter could be deliberately reduced from 1265 to 325 nm during the 15 min of illumination (Figure 2F). After annealing the patterned features at 120 °C for 24 h under argon, a single gold nanoparticle was found within each polymer spot (Figure 2G). Importantly, in accordance with literature precedent, particle size directly correlates with polymer feature size (Figure S3).[10,20c,22] Given that the pen array can be illuminated in a site-selective manner using a focusing lens or other masks,[6] it should be possible to use this technique to generate arrays of nanoparticles with a desired size gradient in a site-controlled manner.

An important aspect of the apertureless pen array approach to on-tip photo-modulated printing is the ability to reverse the properties of the ink after terminating the photoreaction, despite the irreversible nature of the photopolymerization. This is enabled since a reservoir of ink surrounding the base of each pyramid is protected from photopolymerization via an opaque gold layer (Figure 3A and B). To evaluate the effectiveness of the light-blocking layer, the ink-coated pen array after back-side UV illumination (40 min, $\approx 0.1\ mW\,cm^{-2}$) was rinsed with acetone to remove any unreacted NOA ink. SEM images of the rinsed array clearly show solid polymerized NOA ink on the exposed tip, but not in the protected reservoir regions (Figure 3C). The ink in the reservoir regions maintains a low viscosity and can continuously flow towards the tip apex during printing.[23] This is clearly seen in the experiment where NOA ink features were generated via the on-tip photo-modulated molecular printing technique (Figure 3D, top 3 rows) followed by the subsequent generation of similar arrays of features in the dark (Figure 3D, bottom 5 rows). In this set of experiments, the expected feature volume decay was observed in the first three rows due to the light-induced viscosity increase. Once the light has been turned off, the volume of the features gradually increases until reaching a stable value that is comparable to that of the initial feature (Figure 3D and E). This behavior shows that one can use the on-tip photo-modulation to deliberately control ink viscosity at the tip apex by controlling monomer/polymer ratio (Figure 3F). This technique works as long as one does not completely polymerize the monomers and form a solid matrix on the tip. Since diffusion is not instantaneous, the monomer to polymer ink ratio gradually increases after turning off UV illumination. The final feature volume, once equilibrium has been obtained, was found to decrease with increasing extent of polymerization (Figure S4), which is possibly due to a viscosity increase in the reservoir ink that is a consequence of back diffusion of the polymerized ink.

Notably, the reversible change in feature size was not obtained with a conventional PPL array[11] since such architectures do not separate the ink on tip from reservoir

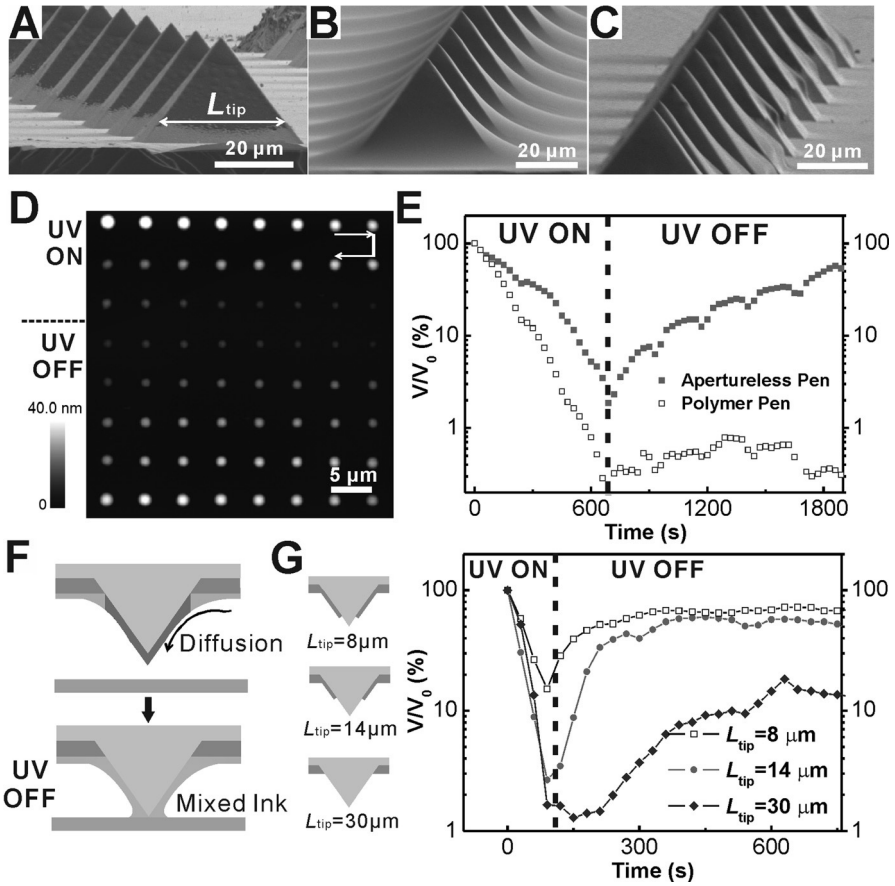

Figure 3. A) SEM image of an apertureless pen array, where L_{tip} represents the edge length of the transparent portion of the tip. B) SEM image of a NOA-coated pen array after front-side UV illumination (40 min, ≈0.1 mW cm^{-2}), showing the ink reservoir around the base of each pyramid deposited by spin coating. C) SEM image of a NOA-coated pen array after back-side UV illumination (40 min, ≈0.1 mW cm^{-2}) and acetone rinsing. D) AFM image of the NOA dot array patterned by the apertureless pen array shown in Figure 3A, with the UV illumination (≈0.1 mW cm^{-2}) applied for the top 3 rows and then switched off for the bottom 5 rows. E) Plot of volume ratio of features ($V/V_0 \times 100$) as a function of time during the patterning process with (left of dashed line) and without (right of dashed line) UV light for apertureless pen (■) and polymer pen (□) arrays. F) Schematic illustration of the on-tip ink diffusion process to dynamically tune the ink properties. G) The effect of L_{tip} on the feature volume ratio change during the patterning over the course of the UV-ON-OFF cycle. The UV intensity is ≈2 mW cm^{-2}.

ink (Figure 3E and S5). We further examined the importance of this apertureless pen architecture and specifically, how the tip's overall surface area affects the change in ink properties by looking at three different arrays with gold layers that not only cover the areas surrounding the base of the tips but also the lower portions of the pyramid (Figure 3A and G). The tips in these three arrays have transparent portions with edge lengths (L_{tip}) of 30, 14 and 8 μm, respectively. Under similar patterning conditions (90 s UV illumination, ≈2 mW cm^{-2}), the pen array with an $L_{tip} = 8$ μm resulted in a slower rate of size decrease compared with the other two, while the pen array with an $L_{tip} = 30$ μm exhibited the slowest rate of size recovery. Effectively, by decreasing the distance from the tip apex to the ink reservoir region (defined by the gold protected layer), the time required for the ink to diffuse to the tip decreases. Therefore, this novel approach provides two important parameters that can be adjusted to control the ink flow, a chemical one (extent of polymerization) and a mechanically controlled one (diffusion distance).

Having shown that the on-tip photopolymerization and ink diffusion can regulate ink transport, we further evaluated the use of the on-tip photochemistry to yield features with modulated chemical functionality through wavelength control. To this end, we took advantage of a reversible photoisomerization reaction to dynamically change ink forms on the tips in situ, without the necessity for changing the pen array or inking procedures. As a proof-of-concept photoisomerization reaction, a closed-ring spiropyran (SP) to open-ring merocyanine (MC) was chosen. The colorless SP can be transformed into a fluorescent MC upon UV irradiation, and this reaction can be reversed with visible light (Figure 4A).[24] In a typical experiment, we printed the spiropyran derivative 1′,3′-dihydro-1′,3′,3′-trimethyl-6-nitrospiro[2*H*-1-benzopyran-2,2′-(2*H*)-indole] with an apertureless pen array using polyethylene glycol (PEG, M_w = 400) as a delivery matrix.[20a] During the patterning process, the light was switched between UV (365 nm, ≈2 mW cm^{-2}) and visible (530 nm, ≈2.5 mW cm^{-2}) wavelengths over 250 s intervals (Figure 4B and D). To study the potential for modulating the composition of the inks and controlling the two molecular forms, we generated a 4×4 dot array, first under UV illumination with a dwell time of 10 s and then an interlaced 3×3 dot array under visible light (Figure 4B inset). The two dot arrays are clearly visible in the dark-field microscopy, while in the fluorescence channel (λ_{ex} = 537–562 nm, λ_{em} = 570–640 nm), only the 4×4 arrays are observed (Figure 4B and S6). This observation is consistent with the UV-induced SP to MC conversion, and the subsequent visible light regeneration of the SP configuration. The switch between SP and MC configurations allows one to reversibly and rapidly change the pattern composition over multiple cycles (Figure 4C and D). Corresponding to the cycling between UV and visible light from row to row, an alternation of weak and strong fluorescence was observed in each row. This fluorescence pattern corresponds to the change in chemical composition of the ink deposited in each row, and it shows that the switch between the two molecular states can be effected within 1 min. It should be noted that the light is confined to the tip, so once a feature has been patterned it is unaffected by the light used thereafter.

In conclusion, this work is important for the following reasons. The introduction of on-tip photo-modulated molecular printing provides both chemically and mechanically controlled approaches to regulating the transport and chemical composition of the ink flow at the tips in real time. This high-throughput dynamic technique, when combined with site-selective light illumination,[6] could enable multiplexed patterning across nano to macro scales for combinatorial screening studies. Given the well-developed field of photochemistry, this approach to photo-modulated feature size and composition could be useful in studying a variety of processes including photoreactions and mass transport at the nanoscale, self-assembly, and cell–material interactions.

Acknowledgements

This material is based upon work supported by the AFOSR under Award FA9550-12-1-0280, National Science Foundation Award DBI-1353682, the General Research Fund of Hong Kong (project PolyU5041/11P), the Natural Science Foundation of China (Project 51273167) and the Hong Kong Polytechnic University (project 4-BCBM). Y.Z. acknowledges Northwestern University for a Ryan Fellowship. J.L.H. was supported by the Department of Defense (DoD) through the National Defense Science & Engineering Graduate Fellowship (NDSEG) Program. This work made use of the EPIC facility (NUANCE Center-Northwestern University), which has received support from the MRSEC program (NSF DMR-1121262) at the Materials Research Center, and the Nanoscale Science and Engineering Center (EEC-0118025/003), both programs of the National Science Foundation; the State of Illinois; and Northwestern University.

Keywords: molecular printing · photochemistry · photocontrol · polymer pen lithography · scanning probe lithography

How to cite: *Angew. Chem. Int. Ed.* **2015**, *54*, 12894–12899
Angew. Chem. **2015**, *127*, 13086–13091

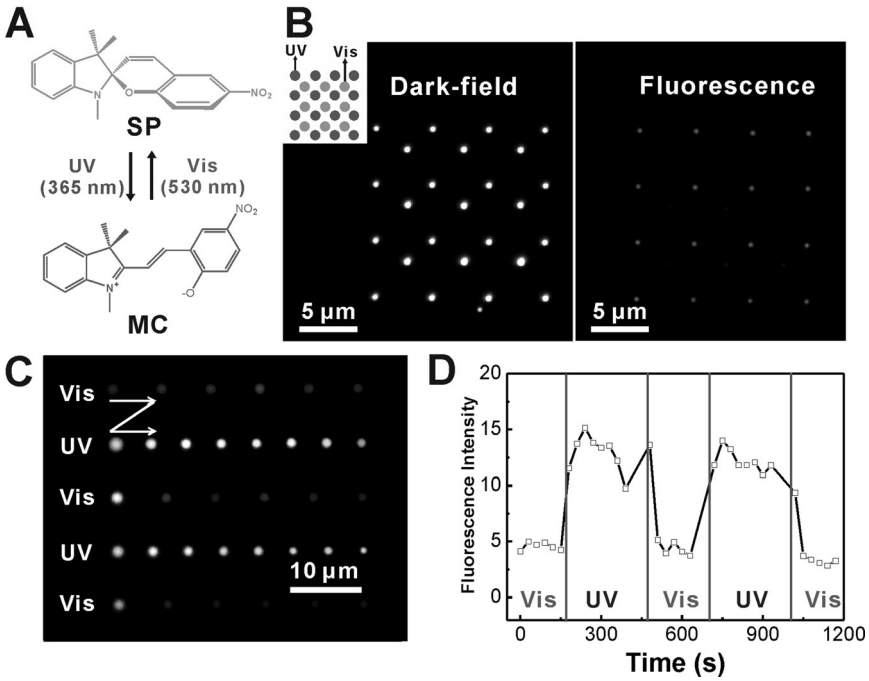

Figure 4. Reversible modulation of ink composition by photoisomerization. A) Schematic illustration of photoisomerization between spiropyran (SP) and merocyanine (MC). The open-ring MC shows intense red fluorescence. B) Dark-field and corresponding fluorescence (λ_{ex} = 537–562 nm, λ_{em} = 570–640 nm) microscope images of two interlaced arrays of PEG/SP ink printed with UV and visible light illumination, respectively. C) Fluorescence microscope image of the printed dot arrays generated while alternating between visible and UV light at the start of each row; the white arrows show the writing direction. Note the first dot in the third and fifth row exhibits fluorescence because the isomerization is not yet complete. D) Plot of fluorescence intensity of the features shown in Figure 4C.

[1] a) K. Salaita, Y. H. Wang, C. A. Mirkin, *Nat. Nanotechnol.* **2007**, *2*, 145–155; b) R. Garcia, A. W. Knoll, E. Riedo, *Nat. Nanotechnol.* **2014**, *9*, 577–587.

[2] a) Z. H. Nie, E. Kumacheva, *Nat. Mater.* **2008**, *7*, 277–290; b) W. F. Maier, K. Stowe, S. Sieg, *Angew. Chem. Int. Ed.* **2007**, *46*, 6016–6067; *Angew. Chem.* **2007**, *119*, 6122–6179; c) A. B. Braunschweig, F. W. Huo, C. A. Mirkin, *Nat. Chem.* **2009**, *1*, 353–358.

[3] a) S. Lenhert, F. Brinkmann, T. Laue, S. Walheim, C. Vannahme, S. Klinkhammer, M. Xu, S. Sekula, T. Mappes, T. Schimmel, H. Fuchs, *Nat. Nanotechnol.* **2010**, *5*, 275–279; b) J. W. Jang, B. Park, S. Nettikadan, *Nanoscale* **2014**, *6*, 7912–7916; c) X. Z. Zhou, Y. Zhou, J. C. Ku, C. Zhang, C. A. Mirkin, *ACS Nano* **2014**, *8*, 1511–1516; d) Y. Zhou, X. Z. Zhou, D. J. Park, K. Torabi, K. A. Brown, M. R. Jones, C. Zhang, G. C. Schatz, C. A. Mirkin, *Nano Lett.* **2014**, *14*, 2157–2161.

[4] a) G. MacBeath, S. L. Schreiber, *Science* **2000**, *289*, 1760–1763; b) N. L. Rosi, C. A. Mirkin, *Chem. Rev.* **2005**, *105*, 1547–1562; c) J. Zhong, M. J. Ma, J. Zhou, D. X. Wei, Z. G. Yan, D. N. He, *ACS Appl. Mater. Interfaces* **2013**, *5*, 737–746.

[5] D. Wouters, U. S. Schubert, *Angew. Chem. Int. Ed.* **2004**, *43*, 2480–2495; *Angew. Chem.* **2004**, *116*, 2534–2550.

[6] a) F. W. Huo, G. F. Zheng, X. Liao, L. R. Giam, J. A. Chai, X. D. Chen, W. Y. Shim, C. A. Mirkin, *Nat. Nanotechnol.* **2010**, *5*, 637–640; b) X. Liao, K. A. Brown, A. L. Schmucker, G. L. Liu, S. He, W. Shim, C. A. Mirkin, *Nat. Commun.* **2013**, *4*, 2103.

[7] S. Xu, S. Miller, P. E. Laibinis, G. Y. Liu, *Langmuir* **1999**, *15*, 7244–7251.

[8] D. Wouters, S. Hoeppener, U. S. Schubert, *Angew. Chem. Int. Ed.* **2009**, *48*, 1732–1739; *Angew. Chem.* **2009**, *121*, 1762–1770.

[9] a) R. D. Piner, J. Zhu, F. Xu, S. H. Hong, C. A. Mirkin, *Science* **1999**, *283*, 661–663; b) D. S. Ginger, H. Zhang, C. A. Mirkin, *Angew. Chem. Int. Ed.* **2004**, *43*, 30–45; *Angew. Chem.* **2004**, *116*, 30–46.

[10] a) J. A. Chai, F. W. Huo, Z. J. Zheng, L. R. Giam, W. Shim, C. A. Mirkin, *Proc. Natl. Acad. Sci. USA* **2010**, *107*, 20202–20206; b) G. L. Liu, D. J. Eichelsdoerfer, B. Rasin, Y. Zhou, K. A. Brown, X. Liao, C. A. Mirkin, *Proc. Natl. Acad. Sci. USA* **2013**, *110*, 887–891.

[11] F. W. Huo, Z. J. Zheng, G. F. Zheng, L. R. Giam, H. Zhang, C. A. Mirkin, *Science* **2008**, *321*, 1658 – 1660.
[12] W. Shim, A. B. Braunschweig, X. Liao, J. Chai, J. K. Lim, G. Zheng, C. A. Mirkin, *Nature* **2011**, *469*, 516 – 521.
[13] a) X. Liu, Y. Li, Z. Zheng, *Nanoscale* **2010**, *2*, 2614 – 2618; b) X. C. Zhou, X. L. Wang, Y. D. Shen, Z. Xie, Z. J. Zheng, *Angew. Chem. Int. Ed.* **2011**, *50*, 6506 – 6510; *Angew. Chem.* **2011**, *123*, 6636 – 6640.
[14] a) P. E. Sheehan, L. J. Whitman, W. P. King, B. A. Nelson, *Appl. Phys. Lett.* **2004**, *85*, 1589 – 1591; b) J. R. Felts, S. Somnath, R. H. Ewoldt, W. P. King, *Nanotechnology* **2012**, *23*, 215301.
[15] a) L. R. Giam, C. A. Mirkin, *Angew. Chem. Int. Ed.* **2011**, *50*, 7482 – 7485; *Angew. Chem.* **2011**, *123*, 7622 – 7625; b) K. A. Brown, D. J. Eichelsdoerfer, W. Shim, B. Rasin, B. Radha, X. Liao, A. L. Schmucker, G. L. Liu, C. A. Mirkin, *Proc. Natl. Acad. Sci. USA* **2013**, *110*, 12921 – 12924; c) Z. Xie, Y. D. Shen, X. C. Zhou, Y. Yang, Q. Tang, Q. Miao, J. Su, H. K. Wu, Z. J. Zheng, *Small* **2012**, *8*, 2664 – 2669; d) M. Xue, X. Cai, G. Chen, *Small* **2015**, *11*, 548 – 552.
[16] a) Z. J. Zheng, W. L. Daniel, L. R. Giam, F. W. Huo, A. J. Senesi, G. F. Zheng, C. A. Mirkin, *Angew. Chem. Int. Ed.* **2009**, *48*, 7626 – 7629; *Angew. Chem.* **2009**, *121*, 7762 – 7765; b) F. Brinkmann, M. Hirtz, A. M. Greiner, M. Weschenfelder, B. Waterkotte, M. Bastmeyer, H. Fuchs, *Small* **2013**, *9*, 3266 – 3275; c) S. D. Bian, J. J. He, K. B. Schesing, A. B. Braunschweig, *Small* **2012**, *8*, 2000 – 2005; d) S. D. Bian, A. M. Scott, Y. Cao, Y. Liang, S. Osuna, K. N. Houk, A. B. Braunschweig, *J. Am. Chem. Soc.* **2013**, *135*, 9240 – 9243; e) X. Han, S. D. Bian, Y. Liang, K. N. Houk, A. B. Braunschweig, *J. Am. Chem. Soc.* **2014**, *136*, 10553 – 10556; f) Z. Xie, C. Chen, X. Zhou, T. Gao, D. Liu, Q. Miao, Z. Zheng, *ACS Appl. Mater. Interfaces* **2014**, *6*, 11955 – 11964.
[17] a) S. Bian, S. B. Zieba, W. Morris, X. Han, D. C. Richter, K. A. Brown, C. A. Mirkin, A. B. Braunschweig, *Chem. Sci.* **2014**, *5*, 2023 – 2030; b) Y. Zhou, Z. Xie, K. A. Brown, D. J. Park, X. Zhou, P.-C. Chen, M. Hirtz, Q.-Y. Lin, V. P. Dravid, G. C. Schatz, Z. Zheng, C. A. Mirkin, *Small* **2015**, *11*, 913 – 918.
[18] X. Liao, A. B. Braunschweig, Z. J. Zheng, C. A. Mirkin, *Small* **2010**, *6*, 1082 – 1086.
[19] a) L. Wang, Z. Zhang, Y. F. Ding, *Soft Matter* **2013**, *9*, 4455 – 4463; b) B. S. Chiou, S. A. Khan, *Macromolecules* **1997**, *30*, 7322 – 7328.
[20] a) L. Huang, A. B. Braunschweig, W. Shim, L. D. Qin, J. K. Lim, S. J. Hurst, F. W. Huo, C. Xue, J. W. Jong, C. A. Mirkin, *Small* **2010**, *6*, 1077 – 1081; b) R. S. Guo, Y. Yu, Z. Xie, X. Q. Liu, X. C. Zhou, Y. F. Gao, Z. L. Liu, F. Zhou, Y. Yang, Z. J. Zheng, *Adv. Mater.* **2013**, *25*, 3343 – 3350; c) G. L. Liu, Y. Zhou, R. S. Banga, R. Boya, K. A. Brown, A. J. Chipre, S. T. Nguyen, C. A. Mirkin, *Chem. Sci.* **2013**, *4*, 2093 – 2099; d) P.-C. Chen, G. Liu, Y. Zhou, K. A. Brown, N. Chernyak, J. L. Hedrick, S. He, Z. Xie, Q.-Y. Lin, V. P. Dravid, S. A. O'Neill-Slawecki, C. A. Mirkin, *J. Am. Chem. Soc.* **2015**, *137*, 9167 – 9173.
[21] D. J. Eichelsdoerfer, K. A. Brown, C. A. Mirkin, *Soft Matter* **2014**, *10*, 5603 – 5608.
[22] J. Wu, X. L. Zan, S. Z. Li, Y. Y. Liu, C. L. Cui, B. H. Zou, W. N. Zhang, H. B. Xu, H. W. Duan, D. B. Tian, W. Huang, F. W. Huo, *Nanoscale* **2014**, *6*, 749 – 752.
[23] a) C. D. O'Connell, M. J. Higgins, D. Marusic, S. E. Moulton, G. G. Wallace, *Langmuir* **2014**, *30*, 2712 – 2721; b) C. D. O'Connell, M. J. Higgins, R. P. Sullivan, S. E. Moulton, G. G. Wallace, *Small* **2014**, *10*, 3717 – 3728.
[24] R. Klajn, *Chem. Soc. Rev.* **2014**, *43*, 148 – 184.

Received: June 5, 2015
Revised: August 3, 2015
Published online: September 9, 2015

